PROCEEDINGS, TOUGH Symposium 2003
Lawrence Berkeley National Laboratory, Berkeley, California, May 12-14, 2003

APPLICATION OF TOUGH2/EWASG TO THE MODELLING OF SALT WATER INJECTION INTO A DEPLETED GEOTHERMAL RESERVOIR: PRELIMINARY RESULTS.

Claudio Calore [1] and Alfredo Battistelli [2]

[1] - Istituto di Geoscienze e Georisorse - CNR
Area della Ricerca CNR, Via G. Moruzzi 1
56124 Pisa, Italy
calore@igg.cnr.it

[2] - Aquater SpA (ENI Group)
Via Miralbello 53
61047 San Lorenzo in Campo (PU), Italy
alfredo.battistelli@aquater.eni.it

ABSTRACT

The TOUGH2/EWASG code is being applied to a numerical study of salt water injection into depleted vapour-dominated geothermal reservoirs. Our study investigates whether the injection of water with a sodium chloride content of 3.3% by weight (similar to that of seawater) for periods of 30 years would lead to conditions of permanent reduction of reservoir permeability, with the consequent negative effects on the recovery of injected fluid as steam. We neglect the effects of water-rock interactions and, in particular, the precipitation of mineral species other than halite, as these are not handled by EWASG. A few test cases were run to investigate the ability of the EWASG V.4 module to solve this type of problem. Numerical experiments have been performed using two-dimensional radial, homogeneous and isotropic porous medium systems with a radius and height of 2 km. Initial conditions were assumed similar to those of some depleted zones of the Larderello and The Geysers reservoirs, which, neglecting the effects of vapour pressure lowering in our models, correspond to single-gas phase conditions. The simulated injection time was 30 years. In this paper we present the preliminary results of one of these models, in which halite precipitation occurs at the vaporization front, and is then followed by dissolution processes taking place when liquid conditions with lower salinity prevail, because of the advancement of the injection plume. Reduction in permeability or sealing of the formation occurs where the injection plume stops propagating, with boiling at its front. Thus, stopping injection would lead to the extension of the zones of the reservoir with reduced permeability or sealed formation all along its final vaporization area. In the model discussed here and throughout the simulated time, there are apparently no evident, negative effects on the recovery of injected brine as steam, because the plume can propagate more or less as if there were no precipitation processes, with about 85% of the injected brine vaporized throughout the simulated 30 years of injection. The results obtained so far have demonstrated the efficacy of the EWASG V.4 module in simulating complex phenomena of coupled mass and heat transport in geothermal reservoirs whose thermodynamic conditions are strongly affected by compositional processes.

INTRODUCTION

As geothermal fluids usually consist of complex mixtures of water, salts, and gases and their thermodynamic and transport properties affect reservoir conditions and performance, the EWASG equation-of-state (EOS) module was developed for the TOUGH2 V.1 multi-purpose numerical reservoir simulator (Pruess, 1991a) to handle three-component fluid mixtures of water, sodium chloride and a slightly soluble non-condensable gas (NCG) (Battistelli et al., 1993; 1997). Apart from low- (Battistelli and Nagy, 2000) and high-temperature (Battistelli et al., 2002) hydrothermal systems, the code can also be applied to the study of underground nuclear waste repositories in saline environments, the unsaturated zone, and environmental problems, such as seawater intrusion into coastal aquifers (Crestaz et al., 2002), and the behaviour of shallow aquifers in volcanic areas. EWASG has been available to the public since 1999 within the TOUGH2 V.2.0 package (Pruess et al., 1999). Minor enhancements to EWASG after 1999 can be found in unpublished reports in Italian.

Using the TOUGH2 V.2.0 with the EWASG V.4 module, we are performing a numerical study to estimate the feasibility of brine injection to recharge depleted vapour-dominated geothermal reservoirs, and at the same time have investigated the ability of the code to simulate this type of problem. Even injection of low salinity brine entails some risk, as it is capable of progressively increasing the salt concentration at the vaporization front, and thus triggering salt precipitation and a consequent reduction in permeability. In our study we investigate whether the injection of water with a sodium chloride content of 3.3% by weight (similar to that of seawater) for periods of the order of tens of

years would lead to conditions of permanent reduction of permeability, with consequent negative effects on the recovery of the injected fluid as steam. Some preliminary results of this study are presented in this paper, as the analysis is still under way.

THE EWASG EOS MODULE

The EWASG EOS module was specifically developed for LBNL's multi-purpose TOUGH2 numerical reservoir simulator, adopting its general structure for coupled multi-phase, multi-component fluids and heat flows (Pruess, 1991a). EWASG was directed at simulating flow problems that include the transport of variable salinity brine and a slightly soluble NCG (Battistelli et al., 1997). Sodium chloride is used to simulate the effects of dissolved salts, whereas the effects of one NCG were included, following a general formulation in which the NCG can be chosen by the user among a set of implemented NCGs. Other NCGs can be easily added by implementing the equations describing their specific thermophysical properties in the existing subroutines. Thus, the multi-phase system is assumed to be composed of three mass components: water, sodium chloride, and an NCG, i.e. carbon dioxide for conventional geothermal applications. The NCGs available in the TOUGH2 V.2.0 package are air, CO_2, CH_4, H_2 and N_2, while O_2 was added in a more recent version of EWASG.

Water and the NCG components may be present in the liquid and gas phases, whereas the salt component may be dissolved in the liquid phase or may have precipitated to form a solid salt phase, which is described in terms of solid saturation, S_s. The adsorption of water or NCG in the solid salt phase is neglected, as well as the small concentration of NaCl in the gas phase. All relevant thermophysical properties are evaluated by means of a subroutine-by-subroutine structure, so that the correlations currently used can be easily modified as soon as more reliable experimental data and correlations become available. The dependence of brine enthalpy, density, viscosity and vapour pressure on salt concentration has been accounted for, as well as the effects of salinity on NCG solubility in the liquid phase and related heat of solution. Vapour pressure lowering caused by suction pressure effects has also been included in the EWASG module. Transport of the mass components occurs by advection in liquid and gas phases, and by molecular diffusion in the gas phase for steam and the NCG, and in the liquid phase for the three components, whereas the modelling of hydrodynamic dispersion has not yet been included in TOUGH2/EWASG. It is assumed that the three phases (gaseous, liquid, and solid) are in local chemical and thermal equilibrium, and that no chemical reactions take place other than interphase mass transfer.

The changes in formation permeability, related to the changes in rock porosity caused by precipitation or dissolution of halite, can be modelled using several alternative porosity-permeability correlations (Verma and Pruess, 1988). These correlations consider idealised models of permeable media in which the pore network is represented by a set of non-intersecting flow channels with either circular tubular or planar cross-sections. Some of these models are able to represent, albeit if in a rough way, the presence of "bottle-necks" in the flow channels. Because of this feature the permeability of the porous medium can drop to zero at a finite porosity, indicated as "critical porosity". For a system of three mass components distributed, according to local thermodynamic equilibrium, over three phases, four independent parameters, or primary variables, are needed to identify the thermodynamic state. In a system of three co-existing phases, seven combinations are possible: three single-phase conditions, three two-phase conditions, and the three-phase condition. With the exclusion of the single-solid salt phase, the EWASG module is able to handle the six remaining phase combinations. Mass balances of water, salt and NCG components, together with the heat balance, are set up and solved by TOUGH2 using the Newton-Raphson iteration method. During the iteration process, the EOS module is able to recognize the appearance and disappearance of phases, including precipitation and dissolution of halite, and to provide all the thermophysical properties of phases present, which are needed to assemble the balance equations.

2-D RADIAL MODELS OF BRINE INJECTION

Brine injection into 1-D radial systems was first modelled to test the numerical behaviour of the code and the accuracy of the numerical solution, because a similarity variable formulation (O'Sullivan, 1981; Pruess et al., 1987) holds in this case. The results were satisfactory, although they pointed out the sensitivity of the solution to space discretization at the vaporization and precipitation fronts.

Numerical experiments were then performed using 2-D radial, homogeneous and isotropic porous medium systems with a radius and height of 2 km, porosity 0.01 and permeability 10^{-14} m^2 (Fig. 1, Table 1). Initial conditions at the top were: total pressure 2.04 MPa, temperature 280°C, and CO_2 partial pressure 0.04 MPa, with gravity equilibrium in the rest of the system. These conditions, neglecting vapour pressure lowering caused by suction pressure effects in our models, correspond to single-gas phase conditions. An initial solid saturation, S_s, of 10^{-6} was assigned throughout the system to limit the execution time, which was strongly affected by the appearance of the solid phase due to halite precipitation at the vaporization front.

The case presented here, Ud, has the characteristics described in Table 2. Corey's relative permeability functions were used, with irreducible liquid saturation S_{lr}=0.80 and irreducible gas saturation S_{gr}=0.05. Capillary pressure effects were introduced using van Genuchten's model (van Genuchten, 1980), with the following parameters: m=0.4438, S_{lr}=0.08, $1/P_0=5.792\cdot10^{-7}$ Pa^{-1}, $P_{max}=5.\cdot10^{7}$ Pa and S_{ls}=1. Molecular diffusion fluxes were considered by computing the effect of phase tortuosity using the Millington and Quirk (1961) model. Diffusion is treated in all phases in a manner that is fully coupled with phase partitioning by using the MOP(24)=0 option. Diffusion coefficients were 10^{-5} m^2/s and 10^{-10} m^2/s for mass components in the gas and liquid phases, respectively. The changes in porosity caused by salt precipitation and the consequent reduction in permeability were modelled by the "tubes-in-series" (Verma and Pruess, 1988), with a critical porosity of 0.008. We chose this high value of critical porosity to cause mass flows to drop to zero, even with a small reduction in pore volume (20%). Active saturations of mobile fluid phases, $S_{la}= S_l/(1-S_s)$ and $S_{ga}=S_g/(1-S_s)$, were used to calculate the capillary pressure and relative permeability of the liquid and gas phases.

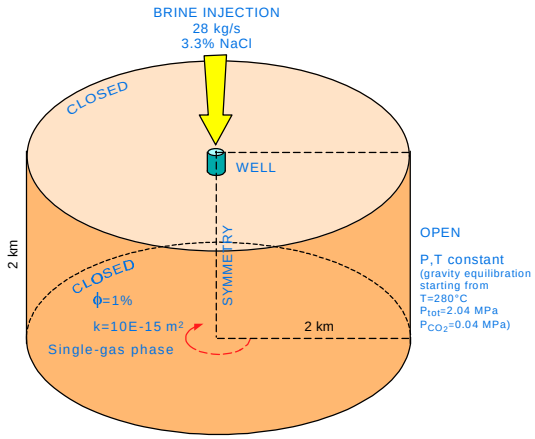

Figure 1. Schematic of the 2-D radial model.

The system was discretized into 40 layers of 50 m thickness, and into 51 columns in the radial direction with width increasing logarithmically from 0.20 m (Fig. 2). The spurious discretization effects on the propagation and shape of the plume, caused by the "rectangular" grid (planar view) used in these simulations, should have been limited by the inclusion of capillary pressure effects in our models (Pruess, 1991b). The simulations were carried out with discretization grid that is coarse enough to use element dimensions that are adequate for field-scale simulations. The injection well was placed at the centre of the system with a 200 m open interval at the top of the reservoir and a radius of 0.20 m. A

Table 1. Parameters common to all simulations.

Formation Parameters	
Rock density	2600 kg/m^3
Porosity	0.01
Thermal conductivity	2.51 W/m°C
Specific heat of rock	1000 J/kg°C
Permeability	10^{-14} m^2
Initial conditions at the top (*)	
Temperature	280°C
Total pressure	2.04 MPa
CO_2 partial pressure	0.04 MPa
Solid saturation	10^{-6}
Injection specifications	
Brine injection rate (96.7% H_2O + 3.3% NaCl)	28 kg/s
Enthalpy	120 kJ/kg

(*) *Gravity equilibrium in the system with top conditions.*

Table 2. Parameters for case Ud.

Relative permeability	Corey	S_{lr}=0.80 S_{gr}=0.05
Capillary pressure	van Genuchten	
Molecular diffusion	Millington and Quirk	
Critical porosity	0.008	

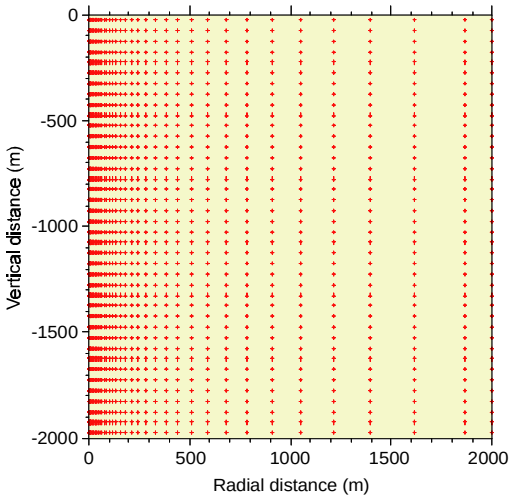

Figure 2. Grid nodes in a vertical half cross-section of the 2-D radial model shown in Fig. 1.

constant brine injection rate of 28 kg/s (96.7% water and 3.3% sodium chloride by weight) was assigned. Constant conditions were maintained at the lateral boundary to simulate the effects of reservoir exploitation, whereas the top and bottom of the

simulated domain were assumed to be impervious and insulated. The simulated injection time was 30 years.

SIMULATION RESULTS

Figure 3 compares the injection plumes, represented by the liquid phase saturation contours, and halite distribution, represented by solid saturation (solid circles) after 10 and 30 years of simulated injection, respectively. Maximum S_s values in the system were 0.198 and 0.206 at 10 and 30 years, respectively.

The plume of liquid brine initially propagates both laterally and vertically due to the injection pressure gradient and the strong suction pressure gradient present at the vaporization front. Density-driven flow due to gravity becomes more and more important with time: when the radial dimension of the plume is such that the injected brine can be drained off across the horizontal section of the plume by density-driven flow, the plume stabilizes in the radial direction and moves downwards only (Calore et al., 1986). Halite precipitation occurs at the vaporization front (Fig. 3), and is then followed by dissolution processes taking place when liquid conditions prevail, thus allowing the vaporization front to proceed. As the liquid brine plume propagates preferentially in the vertical direction at late time, dissolution processes slow down in the radial direction and solid saturation persists alongside the plume, with eventual clogging or even sealing of the formation.

The precipitation/dissolution process was analysed for the grid block 'A5 35' (node coordinates: r=185 m, z=-225 m). Figure 4 shows the plume propagation across 'A5 35'. What occurs when the boiling front of the plume crosses the block is illustrated in greater detail in Figure 5 for 'A5 35' and the upstream grid block 'A5 34' (node coordinates: r=160 m, z=-225 m). Solid salt saturation in 'A5 35' develops when in 'A5 34' the liquid saturation reaches the irreducible saturation value and liquid starts flowing into 'A5 35', where single-gas conditions are initially present. The entering brine completely vaporizes into 'A5 35', thus decreasing temperature in this element, and precipitating sodium chloride. Because of the continuous boiling and liquid supply from the upstream element (S_S in 'A5 35' being even lower than the "critical" value), two-phase conditions are also reached in this element; the liquid phase develops with salt concentration at the equilibrium with halite. As the entering liquid has a lower salt concentration, the halite dissolution process begins and the solid saturation decreases. Once the halite is totally dissolved, the brine is gradually diluted over time, approaching the concentration value of the entering brine from the upstream element, 'A5 34', and finally reaching the injection value. Sealing of

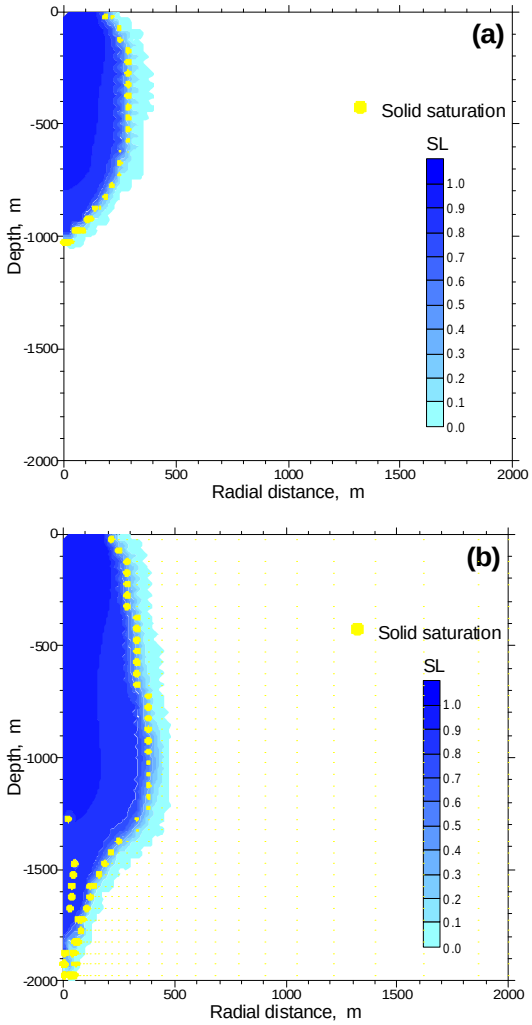

Figure 3. Injection plumes (liquid saturation contours) and distribution of solid saturation in the 2-D radial system after: a) 10 and b) 30 years of simulation time (case Ud).

the formation occurs at the radial boundary of the two-phase region of the plume, because dissolution process ends, being the advancing lower salinity liquid mainly drained off vertically by density-driven flow. The sealing process is shown in Figure 6 for layer 'A5' (225 m depth), together with conditions in the layer within a radius of 400 m at three different times (2, 10 and 30 years, respectively).

Thus, throughout the simulated 30 years of injection, halite precipitation does not cause any damage to reservoir permeability such as to definitively stop the advancement of the vaporization front. The growth trend of the liquid plume is practically linear (Fig. 7), as occurs with pure water injection. After an initial transient, about 85% of the injected fluid continues to vaporize (Fig. 8), sustaining the "production" and the long-term recovery of thermal energy. Steam flows

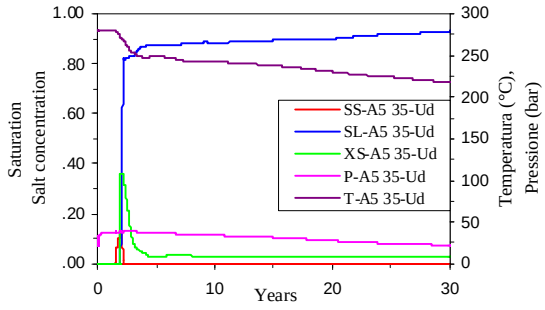

Figure 4. Liquid (SL) and solid (SS) saturations, salt mass fraction (XS), pressure (P) and temperature (T) in the grid block 'A5 35' during 30 years of brine injection.

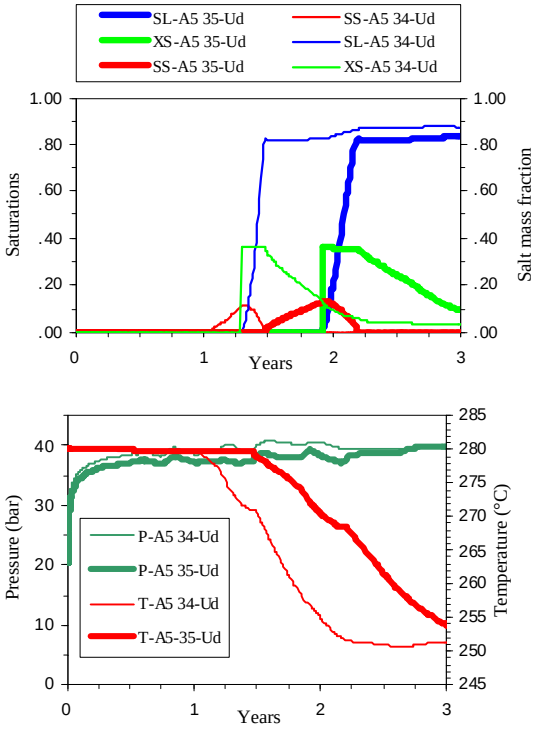

Figure 5. Liquid (SL) and solid (SS) saturations, salt mass fraction (XS), pressure (P) and temperature (T) as the boiling front propagates across the two adjacent grid blocks 'A5 34' and 'A5 35'.

through the constant-pressure lateral boundary at the initial reservoir temperature and at a more or less constant rate of about 23.3 kg/s, which corresponds to 83% of the brine injection rate (Fig. 9).

CONCLUSIONS

A numerical study is under way, using the TOUGH2 V.2.0 with the EWASG V.4 module, to estimate the feasibility of brine injection as a means of recharging

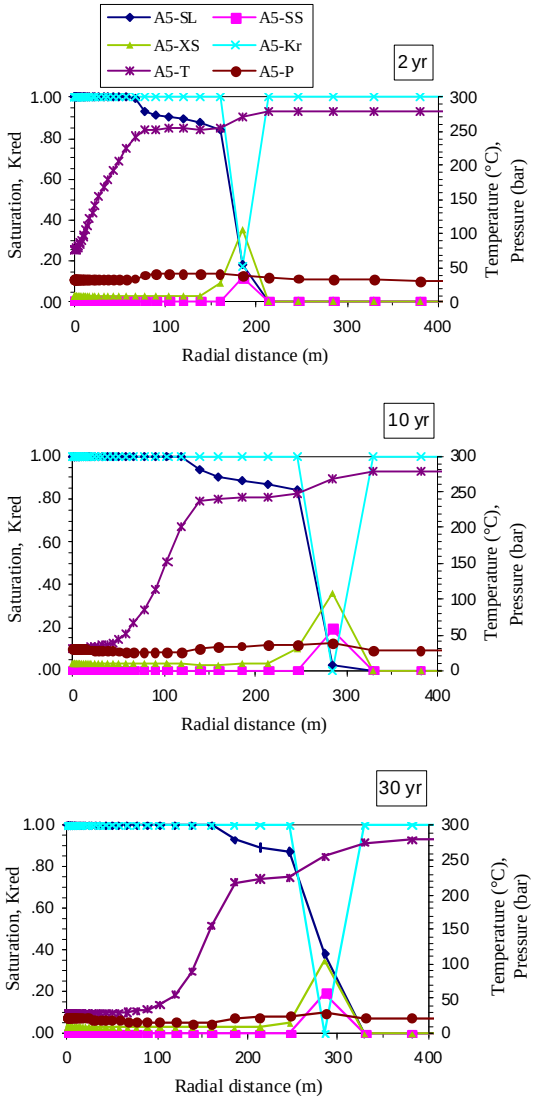

Figure 6. Radial distribution of liquid (SL) and solid (SS) saturations, salt mass fraction (XS), pressure and temperature in the layer 'A5' (depth=225 m) after 2, 10 and 30 years, respectively.

depleted vapour-dominated geothermal reservoirs. We started the numerical experiments using two-dimensional radial, homogeneous and isotropic porous media, with radius and height of 2 km, and initial conditions similar to those of some depleted zones of the Larderello and The Geysers reservoirs, although these systems are characterized by fractured media with low porosity matrix. Neglecting the effects of vapour pressure lowering in our models, these initial conditions correspond to single-gas phase conditions. We neglect the effects of water-rock interactions and, in particular, the precipitation of mineral species other than halite, as these are not included in EWASG. Although the study is still

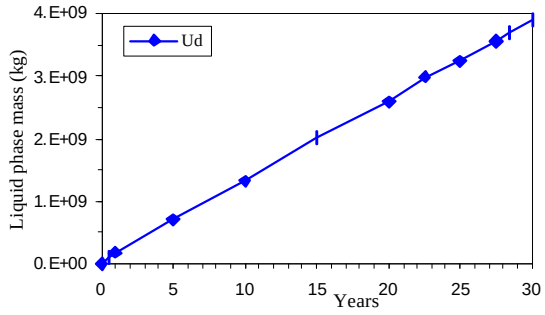

Figure 7. Evolution of the liquid-phase mass present in the reservoir.

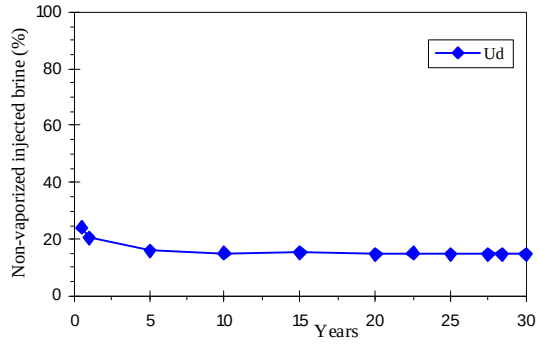

Figure 8. Evolution of the mass fraction (%) of the liquid phase in situ and the cumulative injected fluid.

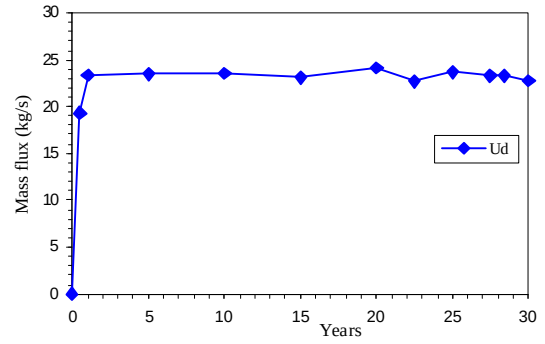

Figure 9. Mass flux across the lateral boundary ("production").

under way and the analysis incomplete, the model discussed here demonstrates that, with the assumptions made, precipitation/dissolution processes do occur, allowing the vaporization front to advance in a way similar to that of the fresh water injection case. Reduction in permeability or sealing of the formation occurs whenever the brine injection plume stops propagating, with boiling at its front. This here occurs at its (upper) radial boundary. In these conditions a halt in injection would lead to a reduction in permeability or sealing of the formation all along its final vaporization area. Throughout the period covered by our simulations there are apparently no negative effects on the recovery of injected fluid as steam, since the plume is able to propagate even in presence of precipitation processes, and about 85% of the injected brine is vaporized throughout the simulated 30 years.

This study has also demonstrated the efficacy of the EWASG V.4 module in simulating complex phenomena of coupled mass and heat transport in geothermal reservoirs whose thermodynamic conditions are strongly affected by compositional processes.

Excluding any analysis of the effects of water-rock interactions and of the precipitation of mineral species other than halite, this study should in future consider:

- brine injection into a fractured-porous medium, representative of superheated geothermal reservoirs, such as Larderello and the Geysers;
- comparison with the case of fresh-water injection;
- the effects of space and time discretization on precipitation/dissolution of halite at the vaporization front;
- different initial reservoir conditions, including vapour pressure lowering phenomena caused by suction pressure effects, which allow the liquid phase to exist even in a depleted vapour-dominated reservoir;
- what occurs when the plume reaches the reservoir bottom;
- enhancement of the EWASG with the inclusion of NaCl solubility in the gas phase, neglected in the present EOS module version, to improve the description of reservoir processes occurring when a high salinity brine is present.

REFERENCES

Battistelli, A., Y. Amdeberhan, C. Calore, C. Ferragina, and A. Wale, Reservoir engineering assessment of Dubti geothermal field, Northern Tendaho Rift, Ethiopia, *Geothermics, 31*(3), 381-406, 2002.

Battistelli, A., C. Calore, and K. Pruess, A fluid property module for the TOUGH2 simulator for saline brines with non-condensible gas, *Proc. 18th Workshop on Geothermal reservoir Engineering*, Stanford University, Stanford, CA, USA, 249-259, 1993.

Battistelli, A., C. Calore, and K. Pruess, The simulator TOUGH2/EWASG for modelling geothermal reservoirs with brines and a non-condensible gas, *Geothermics*, *26*(4), 437-464, 1997.

Battistelli, A., and S. Nagy, Reservoir engineering

assessment of low enthalpy geothermal resources in the Skierniewice-Zyrardow area (Poland), *Geothermics, 29*(6), 701-721, 2000.

Calore, C., K. Pruess, and R. Celati, Modeling studies of cold water injection into fluid-depleted, vapor-dominated geothermal reservoirs, *Proc. 11th Workshop Geothermal Reservoir Engineering, Stanford*, SGP-TR-94, eds. H.J. Ramey et al., *11*, 161-168, 1986.

Crestaz E., H. Adames, A. Battistelli, A. Chersicla, H. Rodriguez, M. Suppo, and L. Tabani, The Planicie Costera Oriental coastal aquifer (Dominican Republic). A general framework analysis supported by conceptual groundwater modelling, *XIV Intl. Conference on Computational Methods in Water Resources*, Delft, The Nederlands, June 23-28, 2002, 546-554, 2002.

Millington, R.J., and J.P. Quirk, Permeability of porous solids, *Trans. Faraday Soc., 57*, 1200-1207, 1961.

O'Sullivan, M.J., A similarity method for geothermal well test analysis, *Water Resour. Res., 17*(2), 390-398, 1981.

Pruess, K., *TOUGH2 - A general-purpose numerical simulator for multi-phase fluid and heat flow*, Report LBL-29400, Lawrence Berkeley Laboratory, Berkeley, Calif., 1991a.

Pruess, K., Grid orientation and capillary pressure effects in the simulation of water injection into depleted vapor zones, *Geothermics, 20*(5/6), 257-277, 1991b.

Pruess, K., C. Calore, R. Celati, and Y. S. Wu, An analytical solution for heat transfer at a boiling front moving through a porous medium, *Int. J. Heat Mass Transfer*, *30*(12), 2595-2602, 1987.

Pruess, K., C. Oldenburg, and G. Moridis, *TOUGH2 User's Guide, Version 2.0*, Report LBNL-43134, Lawrence Berkeley National Laboratory, Berkeley, Calif., 1999.

van Genuchten, M.Th., A closed-form equation for predicting the hydraulic conductivity of unsaturated soils, *Soil Sci. Soc., 44*, 892-898, 1980.

Verma, A., and K. Pruess, Thermohydrological conditions and silica redistribution near high-level nuclear wastes emplaced in saturated geological formations, *Journal of Geophysical Research, 93* (B2), 1159-1173, 19883, 1988.